Journal of Hepatocellular Carcinoma

Dovepress
Taylor & Francis Group

Open Access Full Text Article

ORIGINAL RESEARCH

Nomogram Using Taurocholic Acid, Age, and Albumin to Predict HBV-Related Cirrhosis/HCC in CHB Patients

Xuemei Zhang*, Liming Zheng*, Wenlan Zheng, Jia Shi, Shihan Yu, Hao Liu, Hai Feng*, Zhuo Yu*

Department of Hepatopathy, Shuguang Hospital Affiliated to Shanghai University of Traditional Chinese Medicine, Shanghai, 201203, People's Republic of China

*These authors contributed equally to this work

Correspondence: Zhuo Yu, Department of Hepatopathy, Shuguang Hospital Affiliated to Shanghai University of Traditional Chinese Medicine, 528 Zhangheng Road, Pudong New Area, Shanghai, 201203, People's Republic of China, Tel +86 21 20256507, Fax +86 21 20256699, Email zhuoyu@shutcm.edu.cn

Purpose: Progression to liver cirrhosis (LC) and hepatocellular carcinoma (HCC) is a severe epidemiological risk factor for chronic hepatitis B (CHB); therefore, effective monitoring strategies are urgently required. Dysregulation of bile acids (BAs) metabolism is crucial for aggravating the pathological processes of liver diseases. In this study, we aimed to develop a risk model based on the BAs signature to predict the likelihood of LC and HCC occurrence in CHB patients.

Patients and Methods: A retrospective analysis was conducted using the clinical data of 609 patients diagnosed with CHB, HBV-related LC, and HCC. Patients were randomly assigned to a training or validation set. Logistic regression analyses were employed in the training set to identify key variables and establish a nomogram risk model for predicting the progression of CHB to LC and HCC. Accuracy, calibration, and clinical utility of the model were assessed using a validation set.

Results: Taurocholic acid level and age were independent risk factors, and serum albumin level was a protective factor against the progression of CHB to LC and HCC. A Nomogram risk model was developed using these three indicators, demonstrating a highly accurate and reliable ability to predict the progression from CHB to LC and HCC with good clinical validity and utility.

Conclusion: This study developed a nomogram incorporating BA markers, enabling precise prediction of LC and HCC in patients with CHB. This provided an accurate and accessible method for early screening and prevention.

Keywords: bile acids, chronic hepatitis B, liver cirrhosis, HCC, nomogram

Introduction

Chronic hepatitis B virus (HBV) infection, affecting approximately 296 million individuals worldwide, is the primary cause of liver cirrhosis (LC) and hepatocellular carcinoma (HCC), thus constituting a significant global public health challenge.[1] In 2019, HBV-related LC and HCC were responsible for an estimated 523,000 deaths, and projections indicate that annual global deaths from HBV will increase by 39% between 2015 to 2030.[2,3] Consequently, early detection of LC and HCC is crucial, as it allows for treatments that can either cure the disease or substantially extend patient survival.

The current noninvasive methods for assessing the progression of HBV-related liver disease are notably inadequate. Clinical guidelines recommend several serum indicators, such as aspartate aminotransferase to platelet ratio index (APRI), fibrosis index based on four factors (FIB-4), and alpha-fetoprotein (AFP), for diagnosing LC or HCC. Although these methods are simple and cost-effective, they have significant limitations in terms of sensitivity and specificity.[4–6] Therefore, there is an urgent need for further research to identify new noninvasive biomarkers that can more accurately assess the progression of HBV-related liver disease.

https://doi.org/10.2147/JHC.S559937
Received: 7 September 2025
Accepted: 19 December 2025
Published: 21 January 2026

Graphical Abstract

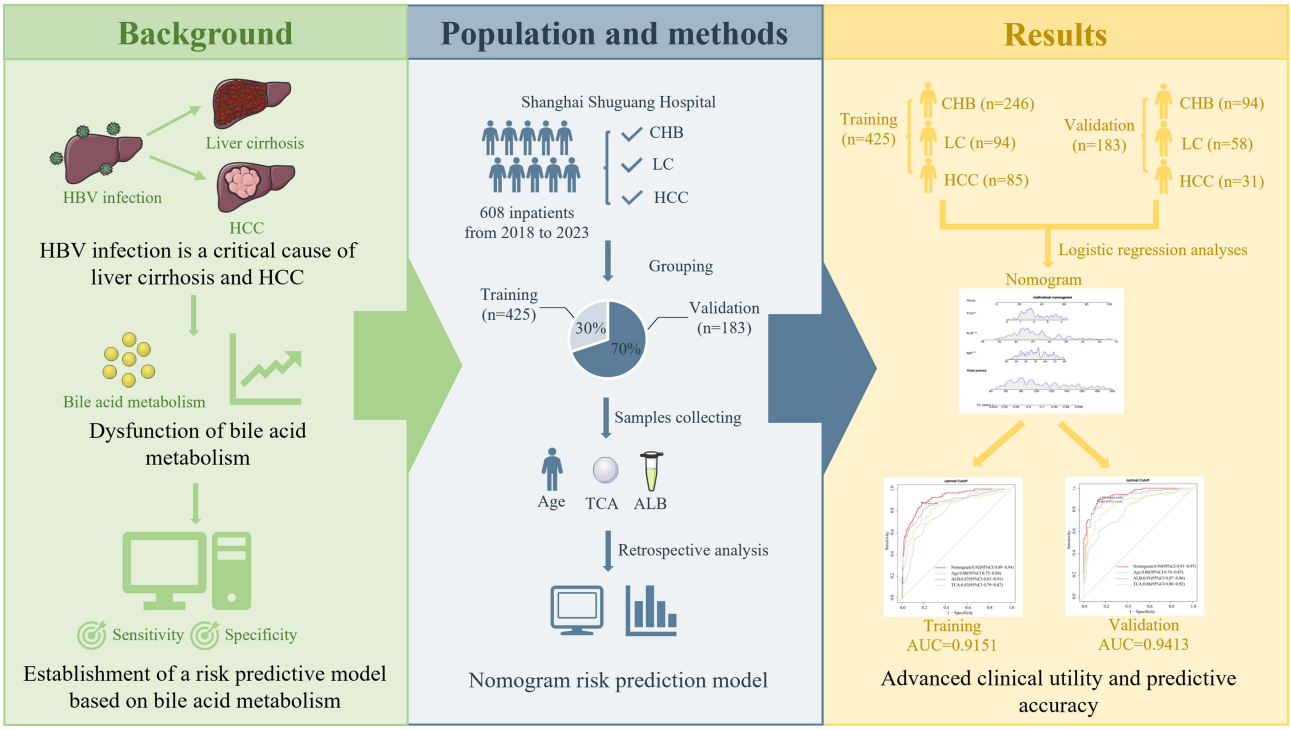

Bile acids (BAs) are the primary metabolites of cholesterol metabolism in the liver and play a pivotal role in regulating lipid, glucose, and energy homeostasis.[7,8] Beyond their physiological functions, BAs also act as signaling molecules that bind to nuclear receptors (eg, farnesoid X receptor, *FXR*) and G protein-coupled receptors (eg, *TGR5*), thereby modulating hepatic inflammation, fibrosis, and carcinogenesis.[9–11] This biological rationale is supported by evidence that HBV infection disrupts hepatocellular BA synthesis, conjugation, and transport, leading to intrahepatic BA accumulation and subsequent activation of profibrotic and pro-oncogenic signaling pathways.[12–14] Recent years have witnessed growing attention on the role of BAs in HBV-related LC and HCC, as several clinical studies demonstrating an association between perturbations in BA composition and the development of HBV-related liver disease.[15–17] However, existing BA-related studies have primarily focused on individual BA species or small panels, lacking systematic characterization of the entire BA metabolic phenotype across the full disease spectrum from CHB to LC and HCC.[7,18–20] Additionally, prior metabolomic studies rarely integrated clinical confounding factors that may alter BA profiles—such as cholestasis (a common complication of advanced liver disease that exacerbates BA dysregulation) and gut microbiota dysbiosis (which modulates secondary BA production via bacterial enzymes like 7α-dehydroxylase)[21–23]—or directly compared the predictive performance of BA-based models with APRI, FIB-4, and AFP in the same cohort.

Understanding the phylogeny of BAs in HBV-related liver diseases is essential for identifying potential biomarkers that can be used to predict and monitor disease progression. Consequently, this retrospective study was conducted to identify BA phenotypes in patients with HBV-related liver diseases, including CHB, LC, and HCC, with the aim of developing a predictive model based on BA metabolism to assess the risk of progression from CHB to LC and HCC.

Materials and Methods

Study Design and Patients

This retrospective analysis utilized data from patients admitted to the Department of Liver Disease at Shuguang Hospital between 2018 and 2023, who were diagnosed with CHB, HBV-related LC, and HCC. Patients were randomly assigned to either the training or validation cohort at a ratio of 7:3 using the R function "Create Data Partition" with a fixed random seed to ensure reproducibility. The training cohort was used to screen variables and construct the prediction model, while the validation cohort was used to internally validate the model performance. Diagnostic criteria were defined as follows: CHB patients were those testing positive for hepatitis B surface antigen (HBsAg) for at least 6 months without evidence of concurrent liver cirrhosis (LC) or hepatocellular carcinoma (HCC).[4] HBV-related LC diagnosis was based on a combination of medical history, physical examination, and results of biochemical tests, endoscopic examination, ultrasound, and enhanced computed tomography (CT)/magnetic resonance imaging (MRI) as per clinical practice.[24] The diagnosis of HBV-related HCC relied on the guidelines of the American Association for the Study of Liver Diseases, including HBsAg positivity, typical imaging features (arterial phase hyperenhancement and venous phase washout) on enhanced CT/MRI, or histological confirmation of malignant hepatocytes via liver biopsy.[25] Exclusion criteria were as follows: 1) Comorbidity with other liver diseases, such as chronic hepatitis C, alcoholic liver disease, nonalcoholic steatohepatitis, autoimmune liver disease, or hereditary liver diseases; 2) Presence of severe complications, including severe infections, acute liver failure, or variceal bleeding; 3) Underlying life-threatening medical conditions, such as acute cardiovascular or cerebrovascular accidents, malignant tumors of other systems, or end-stage renal disease; 4) Patients with severely incomplete clinical or laboratory data (missing key variables including bile acid (BA) profiles, APRI, FIB-4, or AFP).

Sample size calculation: The sample size was determined based on the methods for logistic regression model development, considering the number of potential predictors and expected event rate. A minimum of 10 events per predictor variable was assumed, with the primary outcome defined as progression from CHB to LC/HCC. Based on preliminary data, the expected event rate (proportion of LC/HCC patients) was approximately 40%.[26] We included a series of potential predictors (specially,15 BA species, plus APRI, FIB-4 and AFP), requiring a minimum of 500 events. To account for potential missing data and ensure sufficient statistical power, the final sample size was set at 609 patients, which exceeded the minimum requirement and was consistent with similar metabolomic-based prediction studies in liver diseases.

Ethics Statement

The study was performed in accordance with the ethical standards of the affiliated institutions and the Declaration of Helsinki (2013 revision). The study protocol was reviewed and approved by the Ethics Committee and Institutional Review Board of Shuguang Hospital (No. 2023-1249-16-01). Written informed consent was obtained from each patient prior to enrollment. The consent form, approved by the Shuguang Hospital Ethics Committee, specifically included permission for access to and use of their medical records for this research and for the publication of deidentified findings. For patients unable to provide written consent due to poor health status, consent was obtained from their legal guardians.

Data Collection

Basic clinical data, including demographic information, past medical history, and laboratory features, were extracted from electronic medical records. Demographic and clinical variables included age, sex, duration of HBV infection and history of antiviral treatment (before 3 months of enrollment). Laboratory parameters included: 1) BA profiles (16 key species covering primary/secondary, conjugated/unconjugated BAs); 2) routine blood tests (white blood cell count, neutrophil count, lymphocyte count, platelet count (PLT)); 3) biochemical parameters (alanine aminotransferase (ALT), aspartate aminotransferase (AST), total bilirubin(TBIL), direct bilirubin, albumin(ALB), alkaline phosphatase (ALP), gamma-glutamyl transpeptidase (GGT)); 4) virological parameters (Hepatitis B surface Antigen(HBsAg), hepatitis B e antigen (HBeAg) status, HBV DNA load); 5) serum fibrosis indicators (type IV collagen (CIV), laminin (LN), hyaluronic acid (HA), procollagen III N-terminal peptide (PIIIP)); 6) blood coagulation parameters (prothrombin

time, international normalized ratio (INR)); 7) tumor biomarkers (alpha-fetoprotein (AFP)). Several clinically relevant ratios were calculated: platelet-to-lymphocyte ratio (PLR) = PLT (10^9/L) / lymphocyte count (10^9/L), neutrophil-to-lymphocyte ratio (NLR) = neutrophil count (10^9/L) / lymphocyte count (10^9/L), APRI = (AST / upper limit of normal (ULN)) × 100 / PLT (10^9/L), and FIB-4 = (age × AST) / (PLT × √ALT). Missing data were identified and quantified for each variable. Variables with missing rates < 10% were imputed using the multiple imputation method (with 5 imputed datasets) based on predictive mean matching. Variables with missing rates ≥ 10% were excluded from the final model to avoid bias.

Bile Acid Detection and Pre-Analytical Procedures

Sample collection and processing: Fasting venous blood samples (5 mL) were collected from all patients within 24 hours of admission, centrifuged at 3000 × g for 10 minutes at 4°C to separate serum, and stored at −80°C within 1 hour of collection to avoid BA degradation. Samples were thawed only once before analysis.

Instrument and reagents: BA profiling was performed using an ultra-high-performance liquid chromatography-tandem mass spectrometry (UHPLC-MS/MS) system (Thermo Scientific Ultimate 3000 UHPLC coupled with TSQ Quantis Triple Quadrupole MS, USA). Analytical columns (ACQUITY UPLC BEH C18, 2.1×100 mm, 1.7 μm; Waters, USA) were used for chromatographic separation. Standards of 24 BA species (purity ≥ 98%) were purchased from Sigma-Aldrich (USA), and chromatographic-grade methanol, acetonitrile, and formic acid were obtained from Fisher Scientific (USA).

Chromatographic and mass spectrometric conditions: Mobile phase A consisted of 0.1% formic acid in water, and mobile phase B consisted of 0.1% formic acid in acetonitrile. The gradient elution program was as follows: 0–2 min, 30% B; 2–10 min, 30–90% B; 10–12 min, 90% B; 12–12.1 min, 90–30% B; 12.1–15 min, 30% B. The flow rate was 0.3 mL/min, column temperature was 40°C, and injection volume was 5 μL. MS detection was performed in electrospray ionization (ESI)-negative mode with selected reaction monitoring (SRM). The ion source parameters were: spray voltage = 3500 V, capillary temperature = 320°C, sheath gas pressure = 35 arb, auxiliary gas pressure = 10 arb.

Quality control (QC) and calibration: QC samples were prepared by pooling equal volumes of serum from all patients and analyzed at the beginning, middle, and end of each analytical batch (every 10 samples). The relative standard deviation (RSD) of peak areas for each BA species in QC samples was required to be < 15% to ensure analytical stability. Calibration curves were constructed using serial dilutions of standard solutions (0.01–100 μmol/L) with $R^2 \geq 0.99$. BA concentrations were quantified using external standardization, and results were corrected for matrix effects using the isotope dilution method (stable isotope-labeled cholic acid-d4 and chenodeoxycholic acid-d4 as internal standards).

Statistical Analysis

Quantitative data are presented as mean ± standard deviation (mean ± SD) for normally distributed data or median with interquartile range (M [Q1, Q3]) for non-normally distributed data, whereas categorical variables are expressed as frequency and proportion (n [%]). Data distribution was assessed using the Kolmogorov–Smirnov normality test. For normally distributed data, differences among the three groups (CHB, LC, HCC) were analyzed using one-way analysis of variance (ANOVA) followed by Tukey's post-hoc test; for non-normally distributed data, the Kruskal–Wallis *H*-test followed by Dunn's post-hoc test was used. Categorical variables were compared using the chi-square test or Fisher's exact test (when expected frequencies < 5). To establish the prediction model in the training set, univariate logistic regression analysis was first performed to screen potential predictors ($p < 0.10$). Variables with $p < 0.10$ in univariate analysis were included in multivariate logistic regression with stepwise forward selection (entry criterion: $p = 0.05$; removal criterion: $p = 0.10$). The final model was visualized using a nomogram, with each variable assigned a score based on its regression coefficient. Model evaluation: 1) Discrimination: Assessed by the area under the receiver operating characteristic (ROC) curve (AUC), with 95% confidence intervals (CIs) calculated using the bootstrap method (1000 resamples). AUC values were compared between the BA-based model and traditional indicators (APRI, FIB-4, AFP) using the DeLong test. 2) Calibration: Evaluated by calibration curves, which plot predicted probabilities against observed probabilities, with Hosmer-Lemeshow test ($p > 0.05$ indicating good calibration) and Brier score (lower values indicate better calibration). A calibration plot with 10 equally sized risk groups was generated, and a slope and intercept

correction were applied if necessary. 3) Clinical utility: Assessed by decision curve analysis (DCA) and clinical impact curves (CIC). DCA was used to compare the net benefit of the BA-based model with traditional indicators and the "treat all" or "treat none" strategies across a range of threshold probabilities (0.1–0.9). CIC was used to estimate the number of true positives and false positives at a clinically relevant threshold (preset at 0.3 based on clinical practice and preliminary data). All statistical tests were two-tailed, with a significance level of $p \leq 0.05$. Statistical significance was defined as follows: $*P < 0.05$, $**P < 0.01$, $***P < 0.001$. Statistical analyses were performed using SPSS (V28.0, IBM, USA), R software (V4.3.1, R Foundation for Statistical Computing), and GraphPad Prism (V8.0, GraphPad Software, USA). The nomogram was constructed using the "rms" package in R, and DCA was performed using the "rmda" package.

Results

Baseline Characteristics

A total of 609 eligible patients diagnosed with CHB, HBV-related LC, or HCC between 2018 and 2023 were recruited for this study. The demographic and clinical characteristics of patients are shown in Table 1. The mean ages of patients with CHB, HBV-related LC, and HCC were 44, 59, and 59 years, respectively. The proportions of male patients in the CHB, HBV-related LC, and HCC groups were 78.53%, 53.29%, and 73.28%, respectively. Enrolled patients were randomly

Table 1 Baseline Characteristics of Patients from the Entire Study Population

Variable	Total (n=608)	Group			*P*
		CHB (n=340)	LC (n=152)	HCC (n=116)	
Sex, n (%)					<0.001
Male	433 (71.22)	267 (78.53)	81 (53.29)*	85 (73.28) *	
Female	175 (28.78)	73 (21.47)	71 (46.71)	31 (26.72)	
HBsAg, n (%)					0.263
≤250 (IU/mL)	191 (31.41)	115 (33.82)	46 (30.26)	30 (25.86)	
>250 (IU/mL)	417 (68.59)	225 (66.18)	106 (69.74)	86 (74.14)	
Age (years), M (Q_1, Q_3)	50 (40, 60)	44 (35, 51)	59* (48, 67)	59* (50, 65)	<0.001
HBeAg (IU/mL), M (Q_1, Q_3)	0.39 (0.29, 0.60)	0.40 (0.31, 0.60)	0.38 (0, 0.49)	0.39 (0, 0.86)	0.130
HBcAb (S/CO), M (Q_1, Q_3)	8.87 (7.80, 10.25)	9.27 (8.04, 10.40)	8.74* (7.70, 10.20)	8.11* (7.57, 9.24)	<0.001
AFP (ng/mL), M (Q_1, Q_3)	3.05 (2.19, 5.41)	3.01 (2.32, 4.41)	2.44* (1.71, 4.40)	14.62* (2.94, 158.07)	<0.001
PLR, M (Q_1, Q_3)	67.98 (44.36, 100)	82.68 (60.24, 114.63)	49.61* (31.76, 70.89)	54.21* (38.61, 86.14)	<0.001
NLR, M (Q_1, Q_3)	1.81 (1.25, 2.51)	1.55 (1.12, 2.20)	2.11* (1.54, 2.99)	2.10* (1.64, 3.37)	<0.001
INR, M (Q_1, Q_3)	1.01 (0.93, 1.13)	0.94 (0.90, 0.99)	1.19* (1.06, 1.33)	1.10* (1.04, 1.18)	<0.001
TBIL (umol/L), M (Q_1, Q_3)	15.10 (11.57, 22.45)	12.70 (10.80, 15.90)	21.50* (15.30, 34.20)	20.45* (14.40, 31.03)	<0.001
ALB (umol/L) M (Q_1, Q_3)	41 (36, 43.80)	43.20 (41.30, 45.48)	34.20* (29.20, 39.10)	36.25* (32.30, 39.30)	<0.001
ALT (U/L), M (Q_1, Q_3)	31 (20, 47)	34 (21, 51)	25* (17, 42)	33.50* (22, 47.75)	<0.001
AST (U/L), M (Q_1, Q_3)	34 (23, 51)	37 (25, 56)	28* (19, 42)	35* (22, 46.75)	<0.001
GGT (U/L), M (Q_1, Q_3)	40 (24, 76)	42 (26, 79.50)	29* (18, 47)	51.50* (28, 105.75)	<0.001
ALP (U/L), M (Q_1, Q_3)	80 (65, 101)	72 (63, 87)	87* (71, 118)	100* (78, 157.75)	<0.001
CIV (ng/mL), M (Q_1, Q_3)	63.18 (43.90, 98.54)	53.68 (39.23, 71.60)	95.20* (56.55, 137.70)	90.90* (58, 147.55)	<0.001
LN (ng/mL), M (Q_1, Q_3)	113.37 (87.10, 152)	101.43 (83.91, 124.58)	135.87* (100.47, 202.84)	142.20* (88.57, 210.40)	<0.001
HA, (ng/mL), M (Q_1, Q_3)	149.80 (87.50, 294.79)	118 (71.79, 191.38)	262.21* (104.30, 526.73)	240.02* (127.28, 495.68)	<0.001
PIIIP (ng/mL), M (Q_1, Q_3)	10.20 (7.27, 14.30)	8.75 (6.91, 11.54)	12* (8.56, 18.08)	14.21* (11.01, 19.25)	<0.001
FIB-4, M (Q_1, Q_3)	2.35 (0.84, 3.67)	1.56 (0.97, 2.45)	3.02* (1.39, 4.78)	3.56* (1.53, 4.79)	<0.001
APRI, M (Q_1, Q_3)	0.96 (0.48, 1.53)	0.57 (0.47, 1.39)	1.53 (0.71, 1.86)	1.74 (0.86, 1.98)	0.046

Notes: Quantitative data were presented as median (interquartile range) [M (Q1, Q3)], and were compared using the Kruskal–Wallis test. Categorical variables are presented as n (%) and were compared using the chi-square or Fisher's exact test. All the *p* values were corrected for multiple testing by the Benjamini–Hochberg false discovery rate test. A two-tailed *p* value of <0.05 was considered statistically significant. Significance levels are denoted as follows: $*P < 0.05$.

Abbreviations: CHB, chronic hepatitis B; LC, liver cirrhosis; HCC, hepatocellular carcinoma; APRI, aspartate aminotransferase to platelet ratio index; FIB-4, fibrosis index based on four factors; DCA, decision curves analysis; CIC, clinical impact curves; HBeAg, hepatitis B e antigen; HBsAg, Hepatitis B surface antigen; HBcAb, hepatitis B core-related antibody; AFP, alpha-fetoprotein; PLR, platelet to lymphocyte ratio; NLR, neutrophil to lymphocyte ratio; INR, International normalized ratio; TBIL, total bilirubin; ALB, albumin; ALT, alanine aminotransferase; AST, aspartate aminotransferase; GGT, Serum gamma-glutamyl transferase; ALP, alkaline phosphatase; CIV, collagen IV; LN, laminin; HA, hyaluronic acid; PIIIP, procollagen III peptide; FIB-4, fibrosis-4 index; APRI, aspartate aminotransferase to platelet ratio index.

divided into two cohorts at a ratio of 7:3, resulting in a training cohort of 431 patients and a validation cohort of 178 patients. A detailed flow diagram illustrating the patient selection process is shown in Figure 1. Importantly, there were no significant differences in the clinical variables between the training and validation cohorts (Supplementary Table 1).

The Phenotype of Bile Acid Metabolism in CHB, LC and HCC Patients

We investigated BA metabolism and identified 15 BA-related metabolites in patients with CHB, LC, and HCC using LC-MS on plasma samples from a training cohort comprising 260CHB, 101 LC, and 70 HCC patients (detailed in Supplementary Tables 2 and 4). Notably, significant differences in key clinical metabolic markers were observed between any two of the three groups, except between LC and HCC. As shown in Figure 2A, analysis of BA metabolites across the three groups revealed elevated levels of multiple primary bile acids (PBA) in the LC and HCC groups higher than in the CHB group, whereas levels of multiple secondary bile acids (SBA) were lower in the LC and HCC groups than in the CHB group. Specifically, cholic acid (CA) and chenodeoxycholic acid (CDCA) species were significantly increased in LC and HCC relative to CHB, whereas lithocholic acid (LCA) and deoxycholic acid (DCA) were significantly decreased. Although no statistically significant differences in BA levels were found between LC and HCC, patients with decompensated cirrhosis exhibited significantly higher levels of total BA (TBA), glycocholic acid (GCA), glycochenodeoxycholic acid (GCDCA), taurocholic acid (TCA), taurolithocholic acid (TLCA), taurochenodeoxycholic acid (TCDCA), and tauroursodeoxycholic acid (TUDCA) than those in the compensated stage ($P<0.05$, Supplementary Figures 1A, 2 and 3). To validate our initial findings, we conducted targeted metabolomic profiling of 15 BAs in plasma samples from a validation cohort of 178 participants comprising 84 CHB, 48 LC, and 46 HCC patients. The validation cohort exhibited BA metabolite alterations similar to those observed in the training cohort, with significant upregulation of TBA, GCA, GCDCA, TCDCA, LCA, GUDCA, and TUDCA in both the LC and HCC groups compared with the CHB group (Figure 2B).

To further explore BA metabolism in the gut, we examined the ratio of SBA metabolites to their PBA precursors, as SBA production involves multiple enzymatic reactions facilitated by gut microbiota.[11] Targeted metabolomics revealed a significant decrease in the ratio of DCA to CA in the LC and HCC groups compared with that in the CHB group (Figure 2C). A comparable decrease was noted in the ratio of LCA and UDCA metabolites to CDCA metabolites in the LC and HCC groups compared to that in the CHB group (Figure 2D). These findings suggest that variations in the enzyme activity of the intestinal microbiota contribute to changes in secondary BAs.[27] Additionally, we observed differences in the ratios of circulating conjugated to unconjugated PBAs or SBAs, such as glycine(G)/taurine(T)-DCA /DCA and G/T-LCA/LCA (Figure 2E–H), indicating that imbalances in SBAs are related to enzymatic reactions involving their conjugation with T and G.[27] Furthermore, an increase in the ratio of CA metabolites to CDCA metabolites

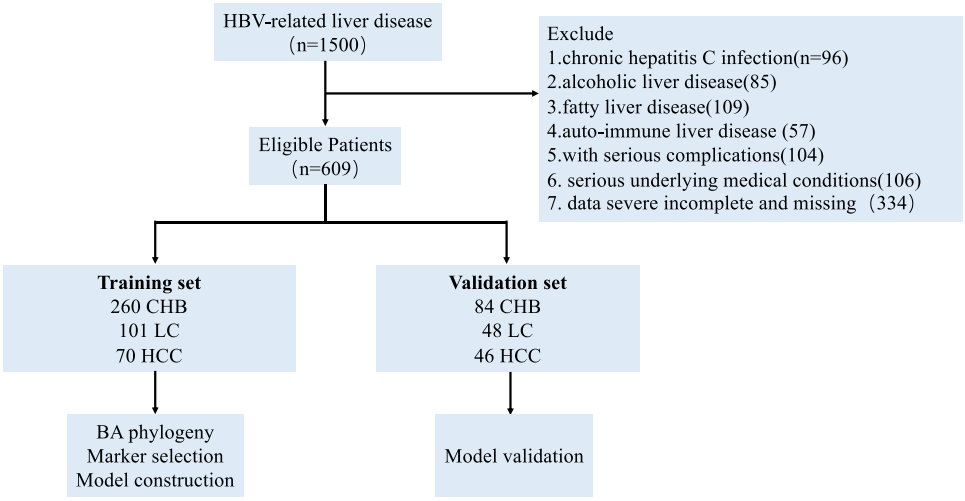

Figure 1 Flow chart of study design and population inclusion and exclusion.

https://doi.org/10.2147/JHC.S559937

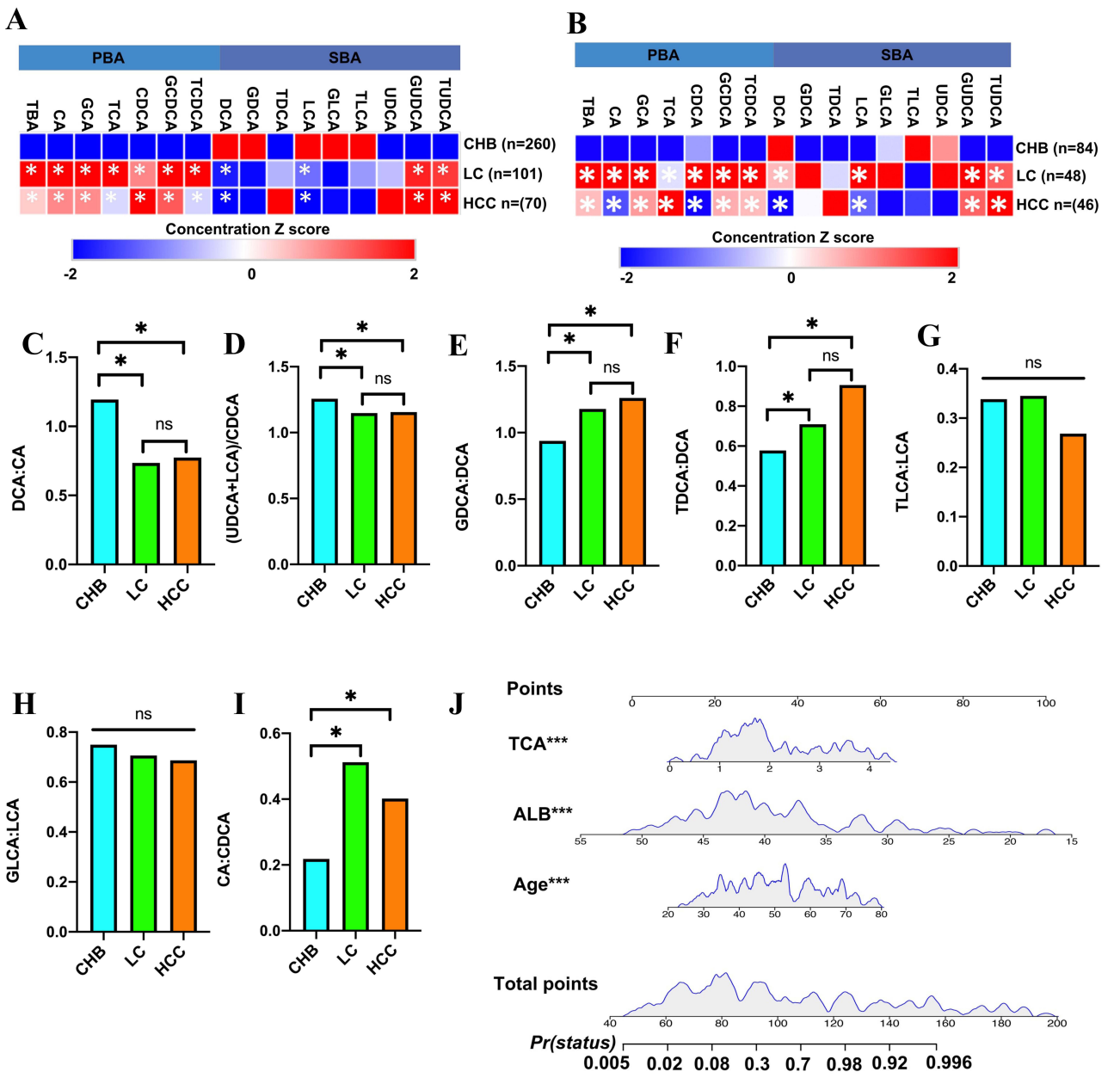

Figure 2 The alteration of bile acid metabolism in CHB, LC and HCC and the Nomogram risk model. (**A**) Heatmap of mean standardized bile acid metabolite concentrations derived from untargeted metabolomic profiling in the discovery cohort consisting of patients with CHB (n = 260), patients with LC (n = 101), and HCC (n = 70). Multiple bile acid metabolites in primary bile acid metabolism pathways were higher in the LC and HCC groups compared with CHB and secondary bile acid metabolism pathways were lower in LC and HCC compared with CHB. Asterisks denote significant differences compared with CHB ($P < 0.05$). (**B**) Heatmap of mean standardized bile acid metabolite concentrations derived from untargeted metabolomic profiling in the validation cohort consisting of patients with CHB (n = 84), patients with LC (n = 48), and HCC (n = 46). Multiple bile acid metabolites in primary bile acid metabolism pathways were higher in the LC and HCC groups compared with CHB and secondary bile acid metabolism pathways were lower in LC and HCC compared with CHB. Asterisks denote significant differences compared with CHB ($P < 0.05$). (**C**) A decrease in the DCA to CA metabolite ratio was noted in the LC and HCC group compared with the CHB group. (**D**) The ratios of (UDCA+LCA) to CDCA metabolites were also lower in the LC and HCC group compared with the CHB group. (**E**–**H**) Changes in the binding of taurine and glycine to secondary bile acids (*$P < 0.05$, **$P < 0.01$, ***$P < 0.001$). (**I**) Bile acid metabolism is mainly maintained in the main pathway. (**J**) A Nomogram risk model for predicting the progression of CHB to cirrhosis and HCC.

was observed in the LC and HCC groups compared to the CHB group (Figure 2I), suggesting a shift in BA synthesis in the liver from the classical pathway to the alternative pathway.[27]

ROC analysis was conducted to evaluate the predictive power of the BAs for the risk of disease progression. The analysis revealed that several BAs, including TBA, CA, CDCA, GCA, GCDCA, TCA, TCDCA, and TUDCA, demonstrated strong predictive capacities in distinguishing HCC and LC from CHB compared to differentiating between HCC and LC. These findings indicate that BAs serve as effective biomarkers for liver disease progression (Supplementary Figure 1B–I).

https://doi.org/10.2147/JHC.S559937

Identification of Risk Factors

We began our analysis with a collinearity test, which led to the exclusion of TUDCA from the logistic regression analysis because of collinearity. Subsequently, we conducted univariate logistic regression analysis incorporating clinical baseline characteristics and BAs as independent variables to identify potential confounders. Univariate analysis revealed several significant variables, including male sex, age, AFP, PLR, NLR, TBIL, ALB, ALP, CIV, LN, HA, PIIIP, FIB-4, TBA, CA, DCA, CDCA, GCA, GCDCA, GUDCA, and TCA (Table 2). These significant variables were then subjected to multivariate logistic regression analysis, which identified TCA, ALB, and age as the independent predictors of disease progression (Table 3 and Supplementary Tables 5 and 6).

Table 2 Predictors of HBV-Related Liver Disease Were Analyzed Using the Univariate Logistic Regression Analysis

Variable	Beta	SE	*Z*	OR (95% CI)	*P*
Male	0.80	0.22	3.70	2.23 (1.46–3.41)	<0.001*
Age	0.10	0.01	9.20	1.10 (1.08–1.12)	<0.001*
AFP	0.01	0.00	2.84	1.01 (1.01–1.02)	0.005*
PLR	−0.01	0.00	−4.91	0.99 (0.98–0.99)	<0.001*
NLR	0.29	0.07	3.93	1.33 (1.15–1.54)	<0.001*
TBIL	0.03	0.01	3.89	1.03 (1.02–1.05)	<0.001*
ALB	−0.35	0.03	−10.17	0.71 (0.66–0.75)	<0.001*
ALP	0.02	0.00	5.32	1.02 (1.01–1.02)	<0.001*
CIV	0.02	0.00	5.67	1.02 (1.01–1.02)	<0.001*
LN	0.01	0.00	5.67	1.01 (1.01–1.02)	<0.001*
HA	0.00	0.00	6.02	1.01 (1.01–1.01)	<0.001*
PIIIP	0.08	0.02	3.95	1.08 (1.04–1.12)	<0.001*
FIB-4	0.73	0.16	4.61	2.07 (1.52–2.82)	<0.001*
TBA	2.04	0.24	8.33	7.65 (4.74–12.35)	<0.001*
CA	1.40	0.19	7.33	4.05 (2.79–5.89)	<0.001*
DCA	−0.36	0.12	−2.94	0.70 (0.55–0.89)	0.003*
CDCA	1.02	0.20	5.13	2.79 (1.88–4.12)	<0.001*
GCA	1.70	0.19	9.13	5.47 (3.80–7.88)	<0.001*
GCDCA	1.93	0.22	8.58	6.88 (4.43–10.69)	<0.001*
GUDCA	0.35	0.10	3.36	1.42 (1.16–1.75)	<0.001*
TCA	1.69	0.17	9.81	5.40 (3.86–7.57)	<0.001*

Note: Significance levels are denoted as follows: *$P < 0.05$.
Abbreviations: AFP, alpha-fetoprotein; PLR, platelet to lymphocyte ratio; NLR, neutrophil to lymphocyte ratio; TBIL, total bilirubin; ALB, albumin; ALP, alkaline phosphatase; CIV, collagen IV; LN, laminin; HA, hyaluronic acid; PIIIP, procollagen III peptide; FIB-4, fibrosis-4 index; TBA, total BA; CA, cholic acid; DCA, deoxycholic acid; CDCA, chenodeoxycholic acid; GCA, glycocholic acid; GCDCA, glycochenodeoxycholic acid; GUDCA, tauroursodeoxycholic acid; TCA, taurocholic acid.

Table 3 Predictors of HBV-Related Liver Disease Were Analyzed Using the Multivariate Logistic Regression Analysis

Variable	Beta	SE	*Z*	OR (95% CI)	*P*
Age	0.09	0.02	4.06	1.09 (1.05–1.14)	<0.001*
ALB	−0.29	0.06	−4.48	0.75 (0.66–0.85)	<0.001*
TCA	2.23	0.47	4.77	9.32 (3.72–23.32)	<0.001*

Note: Significance levels are denoted as follows: *$P < 0.05$.
Abbreviations: ALB, albumin; TCA, taurocholic acid.

Establishment and Validation of the Nomogram Prediction Models

A nomogram prediction model was established based on the risk factors identified through multivariate logistic regression analysis in the training cohort, enabling visual representation of the predictive framework (Figure 2J). The model incorporated three key variables: age, ALB, and TCA. The probability of disease progression in individual patients can be determined by calculating the cumulative points across these variables. In the training set, the model demonstrated excellent discriminative ability, with an AUC value of 0.9151 (95% CI: 0.888–0.9421), achieving a sensitivity of 0.876 and specificity of 0.814 (Figure 3A). The model's robust performance was further confirmed in the validation set, where it achieved an even higher AUC of 0.9413 (95% CI: 0.9096 −0.973), with an enhanced sensitivity (0.895) and specificity (0.86 (Figure 3B). The calibration curves for both sets showed strong alignment with the standard curve, indicating reliable concordance between the predicted probabilities and the observed outcomes (Figure 3C and D). The clinical utility of the model was substantiated by DCA and CIC assessments (Figure 3E–H).

To comprehensively evaluate the predictive advantage of the nomogram, we compared its performance with that of three conventional clinical indicators (APRI, FIB-4, and AFP) in the training cohort. Detailed comparative data are presented in Supplementary Table 3. The nomogram showed the highest AUC (0.915, 95% CI: 0.888–0.942) among all tested indicators, which was significantly superior to APRI (0.610, 95% CI: 0.541–0.678), FIB-4 (0.764, 95% CI: 0.708–0.819), and AFP (0.798, 95% CI: 0.739–0.857). In addition, combined with the optimal cut-off value, sensitivity and specificity, these confirms that the Nomogram has better discriminant power in predicting CHB progression to LC/HCC compared with traditional non-invasive indicators and classical tumor markers AFP.

Discussion

HBV infection is the primary cause of cirrhosis and HCC, with recent statistics indicating incidence rates of 4.91 and 2.57 per 100,000 persons for HBV-related liver cirrhosis and liver cancer, respectively.[1,28] Given that LC and HCC progression develops over time, early recognition and prediction have substantial clinical value. Although noninvasive assessments, including serum biomarkers through laboratory testing, are increasingly being proposed for predicting LC and HCC development, their performance remains controversial. Therefore, it is crucial to identify new indicators of HBV-related LC and HCC progression.

Studies have shown that HBV infection disrupts BAs metabolism.[29,30] As the end products of cholesterol catabolism, BAs act as signaling molecules and metabolic regulators that maintain hepatic lipid, glucose, and energy homeostasis.[8] CA and CDCA PBAs are synthesized in human livers, conjugated with taurine or glycine, and secreted into the intestine.[31] Subsequently, the gut microbiota converts these PBAs into SBAs, including LCA, DCA, and UDCA.[32,33] Excess hepatic BAs can contribute to liver fibrosis, LC, and HCC.[34,35] Given this, we conducted a preliminary validation using serum samples from 609 patients with chronic liver disease (including CHB, HBV-related LC, and HCC) to investigate whether BA indicators can predict HBV-related liver disease progression.

Our analysis revealed significant elevations in CA, GCA, TCA, CDCA, and GCDCA levels in patients with LC and HCC compared with those in the CHB group ($P<0.05$). Conversely, free secondary BAs, DCA, and LCA levels were lower in patients with LC and HCC than in those with CHB group ($P<0.05$). This result was in accordance with that of a previous study, which showed the alterations of some BAs among different stages of hepatitis B, with a decreased conversion of primary to secondary BAs.[36] Therefore, we suspected that primary BAs dehydroxylation might be impaired in HBV-related disease progression because secondary BAs are formed through dehydroxylation of primary BAs catalyzed by bacteria in the intestine.[8] Studies have shown that bacteria involved in BAs metabolism are significantly decreased in CHB- and HBV-induced LC.[36,37] It has been reported that the gut microbiome and HBV-induced chronic liver diseases are linked, and that abnormal BAs circulation caused by the intestinal microbiota may be the reason for CHB progression.[38] The elevation in serum BA levels observed in our study can be partially attributed to cholestasis—a common complication of HBV-related LC and HCC that impairs bile flow and leads to intrahepatic BA accumulation.[39,40]

Even though there was no significant difference in HBV-related LC and HCC in the present study, we found that the levels of BAs, including TBA, GCA, GCDCA, TCA, TLCA, TCDCA, and TUDCA, were significantly increased in patients with LC decompensation compared to the compensated stage, which indicated that BAs were evidently elevated

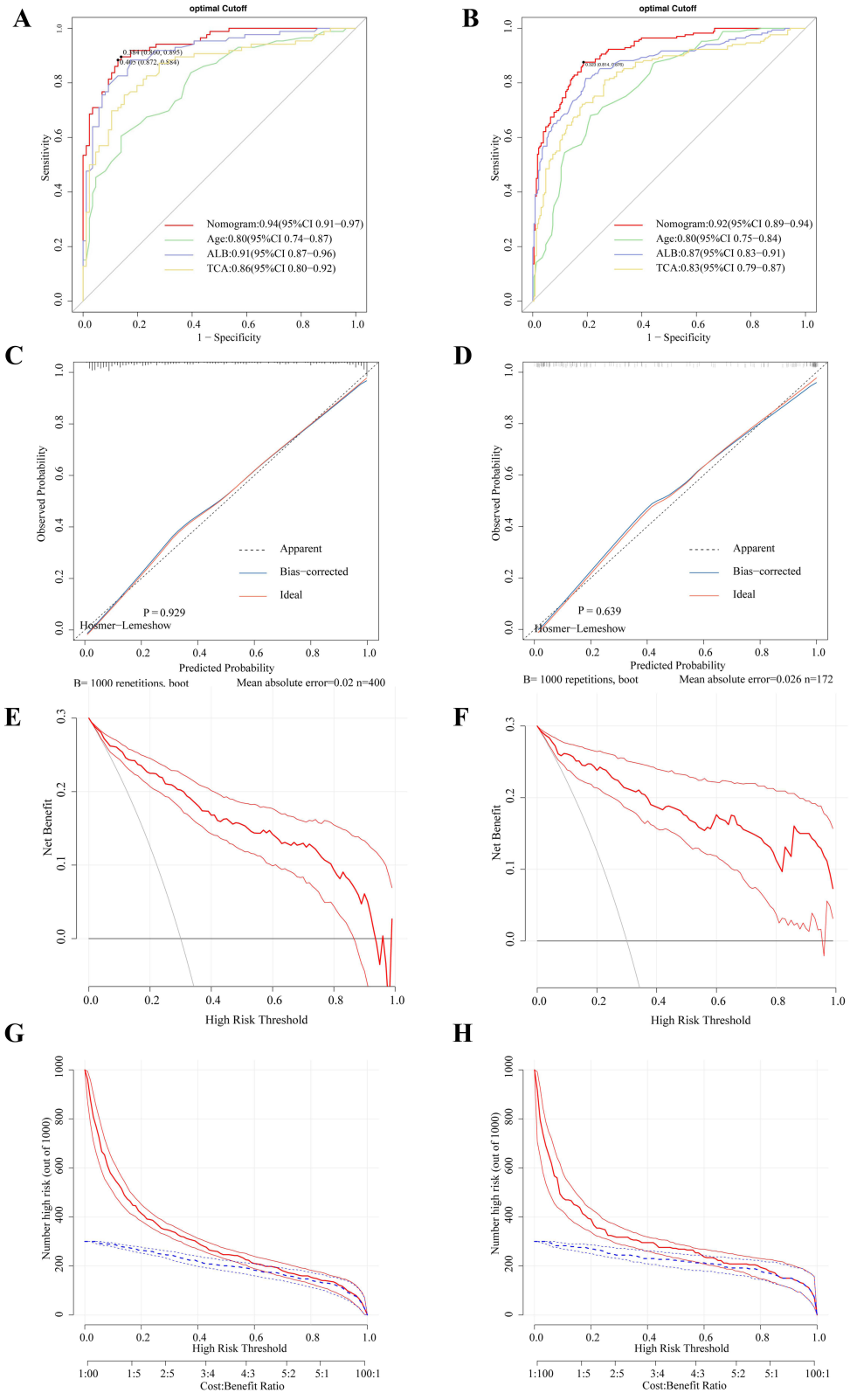

Figure 3 The evaluation and validation of model accuracy and clinical utility. (**A** and **B**) The ROC curve of training and validation cohort. (**C** and **D**) The calibration curves of training and validation cohort. (**E** and **F**) The DCA of training and validation cohort. (**G** and **H**) The CIC of training and validation cohort.

in end-stage liver disease. When hepatitis and cirrhosis progress to HCC, serum levels of GCDCA, TCA, and GCA are elevated.[41] Regarding the indistinct BA trend between LC and HCC, as well as the decreased ROC performance of TCA in distinguishing these two diseases, the core reasons are as follows: ① Pathophysiological overlap between advanced LC and early-to-mid stage HCC, where cirrhosis-driven cholestasis and metabolic disorders mask HCC-specific BA alterations, with TCA elevation primarily driven by cirrhotic dysfunction rather than tumorigenesis itself;[42] ② Biological heterogeneity of HCC (variations in differentiation degree, size/location) leading to overlapping BA profiles with LC;[43,44] ③ Prior clinical interventions (eg, antiviral therapy, hepatoprotective agents) may homogenize BA levels between the two groups, reducing discriminatory efficacy. Collectively, BAs can serve as potential biomarkers for HBV-related liver diseases, such as HBV-related LC and HCC, particularly end-stage liver disease. The above analysis suggests that BAs (especially TCA) are more suitable for assessing liver injury severity and predicting CHB progression to LC/HCC, rather than distinguishing LC from HCC alone. Future studies may combine BA indicators with tumor-specific biomarkers or imaging features to improve discriminatory power.

We confirmed that age, ALB, and TCA were independent factors for the development of HBV-related LC and HCC via univariate and multivariate logistic regression analyses, all of which were significantly correlated with the progression of HBV-related liver disease (all $P<0.001$). Specifically, ALB was associated with a decreased risk, while age and TCA were associated with increased risks of HBV-related LC and HCC. As widely recognized, age and ALB level have been well established as predictors of liver disease progression.[45–47] Notably, our study further identifies elevated serum TCA as an independent risk factor for HBV-related LC or HCC, consistent with the findings of Tan et al,[48] who confirmed TCA as a potential marker for distinguishing HCC from HBV-related chronic liver diseases. Mechanistically, previous studies have demonstrated that high TCA levels promote cirrhotic progression by acting on hepatic cells (eg, hepatic stellate cells and hepatocytes).[49,50] This finding supports the biological rationality of TCA as a predictive biomarker for HBV-related LC and HCC.

Based on these three independent factors, we constructed a predictive nomogram, which exhibited high discrimination and clinical applicability: the area under the curve (AUC) was 0.9151 (95% CI: 0.888–0.9421) in the training set and 0.9413 (95% CI: 0.9096–0.973) in the validation set. Calibration curves, decision curve analysis (DCA), and clinical impact curves (CIC) further verified the reliable predictive accuracy of this model in both cohorts. The nomogram was established with a clinically relevant threshold (sensitivity = 0.663, specificity = 0.84; optimal cutoff value for the nomogram total score: 2.152) to facilitate practical application. Its primary application scenario lies in the early risk stratification of CHB patients during routine clinical surveillance—especially for those with unclear disease progression trends or limited access to advanced imaging examinations—offering a convenient, noninvasive tool to identify high-risk individuals who may require intensified monitoring or intervention. When compared with classical noninvasive indices (APRI, FIB-4) and the gold-standard HCC marker AFP, our nomogram exhibited superior discriminatory power (AUC of nomogram vs APRI: 0.915 vs 0.610; vs FIB-4: 0.915 vs 0.764; vs AFP: 0.915 vs 0.798; all $P < 0.05$), attributed to the integration of TCA, a metabolite directly linked to liver pathophysiology and BAs metabolism dysfunction induced by HBV infection.

We also acknowledge that potential confounding factors may influence the interpretation of our findings: for instance, cholestasis (a common complication in advanced HBV-related liver disease) can independently elevate serum BAs levels, which may partially overlap with the pathogenic effects of TCA on liver fibrosis and carcinogenesis. However, subgroup analysis (data not shown) revealed that the predictive value of TCA remained significant after adjusting for cholestasis-related indicators (eg, total bilirubin, gamma-glutamyl transpeptidase), supporting its independent role beyond mere cholestatic manifestation.

The abnormal BAs profile in our study serves as a predictive biomarker for HBV-related liver disease and identifies potential therapeutic targets to improve BAs metabolism and patient outcomes. First, UDCA, a well-established bile acid replacement therapy for cholestatic liver diseases,[51] inhibits toxic primary BAs synthesis via hepatic CYP7A1 negative feedback.[52] Preclinical and clinical studies confirm UDCA alleviates HBV-induced liver fibrosis,[53] supporting its potential as adjuvant therapy for high-risk individuals. Second, gut microbiota modulation (eg, probiotics) corrects HBV-related BAs imbalance. Due to HBV reducing BAs-dehydroxylating bacteria and impairing primary-to-secondary BAs conversion,[54] Probiotics could restore microbial diversity and BAs dehydroxylation, reversing the imbalance.[55,56]

It is worth noting that numerous prediction models for HCC risk have been reported previously,[57] and as a single-center retrospective study without external validation, the current model may not be immediately translatable to broad clinical practice. However, the integration of TCA (a metabolite with clear biological relevance to liver pathophysiology) with age and ALB provides a novel, concise, and biologically coherent predictive tool that complements existing models—especially given the accessibility of serum TCA detection in clinical settings. The limitations of this study should be acknowledged: first, this was a single-center retrospective cohort study, which may introduce selection bias; second, we did not perform dynamic monitoring of serum bile acid (BAs) levels in patients, and the temporal relationship between TCA changes and disease progression remains to be clarified; third, no prognostic analysis of BAs in HBV-related liver disease was conducted. Therefore, future prospective, large-cohort, multicenter studies are warranted to further validate the value of BAs metabolism (especially TCA) in the prognosis of HBV-related liver disease and to perform external validation of the proposed nomogram. Additionally, in vitro cellular and in vivo animal experiments are needed to further elucidate the underlying molecular mechanisms by which BAs metabolism regulates HBV-related liver disease progression.

Conclusion

Our results provided preliminary evidences for BAs to be used as biomarkers for the HBV-related liver disease, and developed a Nomogram enabling precise prediction of LC and HCC in CHB patients. This nomogram provides an accurate and accessible method for early screening and prevention, potentially improving routine surveillance and prediction of HBV-related LC or HCC in clinical practice. However, prospective, multicenter, large-cohort studies are needed to validate the model further, which will assist clinicians in timely and accurate identification of high-risk CHB patients for targeted prevention and personalized management.

Ethics Approval and Consent to Participate

The study was performed in accordance with the ethical standards of the institutions affiliated with the Declaration of Helsinki (as revised in 2013). Written informed consent was obtained from the patient for publication of this case report and accompanying images.

Acknowledgments

The authors acknowledge all the clinical staff from the department and laboratory.

Author Contributions

All authors made a significant contribution to the work reported, whether that is in the conception, study design, execution, acquisition of data, analysis and interpretation, or in all these areas; took part in drafting, revising or critically reviewing the article; gave final approval of the version to be published; have agreed on the journal to which the article has been submitted; and agree to be accountable for all aspects of the work.

Funding

This work was supported by grants from National Natural Science Foundation of China (82574750, 82222074, 82074154), Shuguang Program of Shanghai Education Development Foundation and Shanghai Municipal Education Commission (23SG38), Youth Tip-top Talent program in Shanghai, High Level Key Discipline of the State Administration of Traditional Chinese Medicine (ZYYZDXK-2023060), Shanghai Key Laboratory of Traditional Chinese Clinical Medicine (20DZ2272200).

Disclosure

The author(s) report no conflicts of interest in this work.

References

1. Veracruz N, Gish RG, Cheung R, et al. Global incidence and mortality of hepatitis B and hepatitis C acute infections, cirrhosis and hepatocellular carcinoma from 2010 to 2019. *J Viral Hepat*. 2022;29:352–365. doi:10.1111/jvh.13663

2. Noverati N, Bashir-Hamidu R, Halegoua-DeMarzio D, et al. Hepatitis B virus-associated hepatocellular carcinoma and chronic stress. *Int J Mol Sci*. 2022;23:3917. doi:10.3390/ijms23073917
3. Razavi-Shearer D, Gamkrelidze I, Nguyen MH, et al. Global prevalence, treatment, and prevention of hepatitis B virus infection in 2016: a modelling study. *Lancet Gastroenterol Hepatol*. 2018;3:383–403. doi:10.1016/S2468-1253(18)30056-6
4. Terrault NA, Lok ASF, McMahon BJ, et al. Update on prevention, diagnosis, and treatment of chronic hepatitis B: AASLD 2018 hepatitis B guidance. *Hepatology*. 2018;67:1560–1599. doi:10.1002/hep.29800
5. Terrault NA, Bzowej NH, Chang KM, et al. AASLD guidelines for treatment of chronic hepatitis B. *Hepatology*. 2016;63:261–283. doi:10.1002/hep.28156
6. Kim WR, Berg T, Asselah T, et al. Evaluation of APRI and FIB-4 scoring systems for non-invasive assessment of hepatic fibrosis in chronic hepatitis B patients. *J Hepatol*. 2016;64:773–780. doi:10.1016/j.jhep.2015.11.012
7. Sun R, Zhang Z, Bao R, et al. Loss of SIRT5 promotes bile acid-induced immunosuppressive microenvironment and hepatocarcinogenesis. *J Hepatol*. 2022;77:453–466. doi:10.1016/j.jhep.2022.02.030
8. Chiang JY. Bile acid metabolism and signaling. *Compr Physiol*. 2013;3:1191–1212. doi:10.1002/j.2040-4603.2013.tb00517.x
9. Zhang L, Wu GY, Wu YJ, et al. The serum metabolic profiles of different Barcelona stages hepatocellular carcinoma associated with hepatitis B virus. *Oncol Lett*. 2018;15:956–962. doi:10.3892/ol.2017.7393
10. Han X, Wang J, Gu H, et al. Predictive value of serum bile acids as metabolite biomarkers for liver cirrhosis: a systematic review and meta-analysis. *Metabolomics*. 2022;18:43. doi:10.1007/s11306-022-01890-y
11. Zhang X, Shi L, Lu X, et al. Bile acids and liver cancer: molecular mechanism and therapeutic prospects. *Pharmaceuticals*. 2024;17:1142. doi:10.3390/ph17091142
12. Yin P, Wan D, Zhao C, et al. A metabonomic study of hepatitis B-induced liver cirrhosis and hepatocellular carcinoma by using RP-LC and HILIC coupled with mass spectrometry. *Mol Biosyst*. 2009;5:868–876. doi:10.1039/b820224a
13. Wang H, Shang X, Wan X, et al. Increased hepatocellular carcinoma risk in chronic hepatitis B patients with persistently elevated serum total bile acid: a retrospective cohort study. *Sci Rep*. 2016;6:38180. doi:10.1038/srep38180
14. Zhang W, Zhou L, Yin P, et al. A weighted relative difference accumulation algorithm for dynamic metabolomics data: long-term elevated bile acids are risk factors for hepatocellular carcinoma. *Sci Rep*. 2015;5:8984. doi:10.1038/srep08984
15. Song Y, Lau HC, Zhang X, et al. Bile acids, gut microbiota, and therapeutic insights in hepatocellular carcinoma. *Cancer Biol Med*. 2023;21:144–162. doi:10.20892/j.issn.2095-3941.2023.0394
16. Yoshimoto S, Loo TM, Atarashi K, et al. Obesity-induced gut microbial metabolite promotes liver cancer through senescence secretome. *Nature*. 2013;499:97–101. doi:10.1038/nature12347
17. Stepien M, Lopez-Nogueroles M, Lahoz A, et al. Prediagnostic alterations in circulating bile acid profiles in the development of hepatocellular carcinoma. *Int J Cancer*. 2022;150:1255–1268. doi:10.1002/ijc.33885
18. Conde de la Rosa L, Garcia-Ruiz C, Vallejo C, et al. STARD1 promotes NASH-driven HCC by sustaining the generation of bile acids through the alternative mitochondrial pathway. *J Hepatol*. 2021;74:1429–1441. doi:10.1016/j.jhep.2021.01.028
19. Ji G, Si X, Dong S, et al. Manipulating liver bile acid signaling by nanodelivery of bile acid receptor modulators for liver cancer immunotherapy. *Nano Lett*. 2021;21:6781–6791. doi:10.1021/acs.nanolett.1c01360
20. Ma C, Han M, Heinrich B, et al. Gut microbiome-mediated bile acid metabolism regulates liver cancer via NKT cells. *Science*. 2018;360. doi:10.1126/science.aan5931
21. Shen R, Ke L, Li Q, et al. Abnormal bile acid-microbiota crosstalk promotes the development of hepatocellular carcinoma. *Hepatol Int*. 2022;16:396–411. doi:10.1007/s12072-022-10299-7
22. Nobel YR, Park H, Tillman AM, et al. Fecal microbiota and bile acid profiles in early-stage hepatocellular carcinoma: a matched case-control study. *Clin Transl Gastroenterol*. 2025;16:e00928. doi:10.14309/ctg.0000000000000928
23. Jacobs JP, Dong TS, Agopian V, et al. Microbiome and bile acid profiles in duodenal aspirates from patients with liver cirrhosis: the microbiome, microbial markers and liver disease study. *Hepatol Res*. 2018;48:1108–1117. doi:10.1111/hepr.13207
24. Yoshiji H, Nagoshi S, Akahane T, et al. Evidence-based clinical practice guidelines for Liver Cirrhosis 2020. *J Gastroenterol*. 2021;56:593–619. doi:10.1007/s00535-021-01788-x
25. Xie DY, Ren ZG, Zhou J, et al. 2019 Chinese clinical guidelines for the management of hepatocellular carcinoma: updates and insights. *Hepatobiliary Surg Nutr*. 2020;9:452–463. doi:10.21037/hbsn-20-480
26. Kim HY, Lampertico P, Nam JY, et al. An artificial intelligence model to predict hepatocellular carcinoma risk in Korean and Caucasian patients with chronic hepatitis B. *J Hepatol*. 2022;76:311–318. doi:10.1016/j.jhep.2021.09.025
27. MahmoudianDehkordi S, Arnold M, Nho K, et al. Altered bile acid profile associates with cognitive impairment in Alzheimer's disease-An emerging role for gut microbiome. *Alzheimers Dement*. 2019;15:76–92. doi:10.1016/j.jalz.2018.07.217
28. Gilles H, Garbutt T, Landrum J. Hepatocellular Carcinoma. *Crit Care Nurs Clin North Am*. 2022;34:289–301. doi:10.1016/j.cnc.2022.04.004
29. Oehler N, Volz T, Bhadra OD, et al. Binding of hepatitis B virus to its cellular receptor alters the expression profile of genes of bile acid metabolism. *Hepatology*. 2014;60:1483–1493. doi:10.1002/hep.27159
30. Tanaka N, Matsubara T, Krausz KW, et al. Disruption of phospholipid and bile acid homeostasis in mice with nonalcoholic steatohepatitis. *Hepatology*. 2012;56:118–129. doi:10.1002/hep.25630
31. Jia W, Xie G, Jia W. Bile acid-microbiota crosstalk in gastrointestinal inflammation and carcinogenesis. *Nat Rev Gastroenterol Hepatol*. 2018;15:111–128. doi:10.1038/nrgastro.2017.119
32. Goossens JF, Bailly C. Ursodeoxycholic acid and cancer: from chemoprevention to chemotherapy. *Pharmacol Ther*. 2019;203:107396. doi:10.1016/j.pharmthera.2019.107396
33. Ridlon JM, Kang DJ, Hylemon PB. Bile salt biotransformations by human intestinal bacteria. *J Lipid Res*. 2006;47:241–259. doi:10.1194/jlr.R500013-JLR200
34. Liu Y, Chen K, Li F, et al. Probiotic Lactobacillus rhamnosus GG prevents liver fibrosis through inhibiting hepatic bile acid synthesis and enhancing bile acid excretion in mice. *Hepatology*. 2020;71:2050–2066. doi:10.1002/hep.30975
35. Anakk S, Bhosale M, Schmidt VA, et al. Bile acids activate YAP to promote liver carcinogenesis. *Cell Rep*. 2013;5:1060–1069. doi:10.1016/j.celrep.2013.10.030

36. Wang X, Chen L, Wang H, et al. Modulation of bile acid profile by gut microbiota in chronic hepatitis B. *J Cell Mol Med*. 2020;24:2573–2581. doi:10.1111/jcmm.14951
37. Lu H, Wu Z, Xu W, et al. Intestinal microbiota was assessed in cirrhotic patients with hepatitis B virus infection. Intestinal microbiota of HBV cirrhotic patients. *Microb Ecol*. 2011;61:693–703. doi:10.1007/s00248-010-9801-8
38. Hasegawa S, Yoneda M, Kurita Y, et al. Cholestatic liver disease: current treatment strategies and new therapeutic agents. *Drugs*. 2021;81:1181–1192. doi:10.1007/s40265-021-01545-7
39. Cao X, Gao Y, Zhang W, et al. Cholestasis morbidity rate in first-hospitalized patients with chronic liver disease in Shanghai. *Zhonghua Gan Zang Bing Za Zhi*. 2015;23:569–573. doi:10.3760/cma.j.issn.1007-3418.2015.08.003
40. Lo RC, Kim H. Histopathological evaluation of liver fibrosis and cirrhosis regression. *Clin Mol Hepatol*. 2017;23:302–307. doi:10.3350/cmh.2017.0078
41. Chen T, Xie G, Wang X, et al. Serum and urine metabolite profiling reveals potential biomarkers of human hepatocellular carcinoma. *Mol Cell Proteomics*. 2011;10:M110.004945. doi:10.1074/mcp.M110.004945
42. Ma J, Cheng M, Jin L, et al. Comprehensive multi-omics analysis of bile acid metabolism in hepatocellular carcinoma: implications for prognosis, immune microenvironment, and therapeutic resistance. *Clin Transl Oncol*. 2025;27:4430–4449. doi:10.1007/s12094-025-03963-5
43. Sydor S, Best J, Messerschmidt I, et al. Altered microbiota diversity and bile acid signaling in cirrhotic and noncirrhotic NASH-HCC. *Clin Transl Gastroenterol*. 2020;11:e00131. doi:10.14309/ctg.0000000000000131
44. Xing L, Zhang Y, Li S, et al. A dual coverage monitoring of the bile acids profile in the liver-gut axis throughout the whole inflammation-cancer transformation progressive: reveal hepatocellular carcinoma pathogenesis. *Int J Mol Sci*. 2023;24:4258. doi:10.3390/ijms24054258
45. Yang H, Bae SH, Nam H, et al. A risk prediction model for hepatocellular carcinoma after hepatitis B surface antigen seroclearance. *J Hepatol*. 2022;77:632–641. doi:10.1016/j.jhep.2022.03.032
46. Spinella R, Sawhney R, Jalan R. Albumin in chronic liver disease: structure, functions and therapeutic implications. *Hepatol Int*. 2016;10:124–132. doi:10.1007/s12072-015-9665-6
47. Yang YT, Jiang JH, Yang HJ, et al. The lymphocyte-to-monocyte ratio is a superior predictor of overall survival compared to established biomarkers in HCC patients undergoing liver resection. *Sci Rep*. 2018;8:2535. doi:10.1038/s41598-018-20199-2
48. Tan Y, Yin P, Tang L, et al. Metabolomics study of stepwise hepatocarcinogenesis from the model rats to patients: potential biomarkers effective for small hepatocellular carcinoma diagnosis. *Mol Cell Proteomics*. 2012;11:M111.010694. doi:10.1074/mcp.M111.010694
49. Pozniak KN, Pearen MA, Pereira TN, et al. Taurocholate induces biliary differentiation of liver progenitor cells causing hepatic stellate cell chemotaxis in the ductular reaction: role in pediatric cystic fibrosis liver disease. *Am J Pathol*. 2017;187:2744–2757. doi:10.1016/j.ajpath.2017.08.024
50. Liu Z, Zhang Z, Huang M, et al. Taurocholic acid is an active promoting factor, not just a biomarker of progression of liver cirrhosis: evidence from a human metabolomic study and in vitro experiments. *BMC Gastroenterol*. 2018;18:112. doi:10.1186/s12876-018-0842-7
51. Paumgartner G, Beuers U. Mechanisms of action and therapeutic efficacy of ursodeoxycholic acid in cholestatic liver disease. *Clin Liver Dis*. 2004;8:67–81, vi. doi:10.1016/S1089-3261(03)00135-1
52. Johansson H, Mörk LM, Li M, et al. Circulating fibroblast growth factor 19 in portal and systemic blood. *J Clin Exp Hepatol*. 2018;8:162–168. doi:10.1016/j.jceh.2017.07.001
53. He H, Mennone A, Boyer JL, et al. Combination of retinoic acid and ursodeoxycholic acid attenuates liver injury in bile duct-ligated rats and human hepatic cells. *Hepatology*. 2011;53:548–557. doi:10.1002/hep.24047
54. Sun Z, Huang C, Shi Y, et al. Distinct bile acid profiles in patients with chronic hepatitis B virus infection reveal metabolic interplay between host, virus and gut microbiome. *Front Med*. 2021;8:708495. doi:10.3389/fmed.2021.708495
55. Xun Z, Yao X, Lin C, et al. A novel therapy targeting the gut-liver axis for chronic hepatitis B: ursodeoxycholic acid plus Bifidobacterium. *JHEP Rep*. 2025;7:101456. doi:10.1016/j.jhepr.2025.101456
56. Liu W, Li Z, Ze X, et al. Multispecies probiotics complex improves bile acids and gut microbiota metabolism status in an in vitro fermentation model. *Front Microbiol*. 2024;15:1314528. doi:10.3389/fmicb.2024.1314528
57. Nahon P, Bamba-Funck J, Layese R, et al. Integrating genetic variants into clinical models for hepatocellular carcinoma risk stratification in cirrhosis. *J Hepatol*. 2023;78:584–595. doi:10.1016/j.jhep.2022.11.003